

Raman scattering study of CaB_6 and YbB_6

Norio Ogita,^{a,*} Shinji Nagai,^a Naoki Okamoto,^a Fumitoshi Iga,^b Satoru Kunii,^c
Toshiro Akamitsu,^d Jun Akimitsu,^d and Masayuki Udagawa^a

^a Faculty of Integrated Arts and Sciences, Hiroshima University, Higashi, Hiroshima 739-8521, Japan

^b Graduate School of Advanced Sciences of Matter, Hiroshima University, Hiroshima 739-8530, Japan

^c Department of Physics, Graduate School of Science, Tohoku University, Sendai 980-8578, Japan

^d Department of Physics, Aoyama-Gakuin University, Tokyo 157-8521, Japan

Received 30 September 2002; accepted 12 February 2003

Abstract

Phonon spectra of CaB_6 and RB_6 ($R = \text{Yb, Ce, and Pr}$) have been investigated by Raman scattering. We found clear spectral difference between divalent cation hexaboride and trivalent one. E_g mode shows the doublet spectra for only the divalent crystals of CaB_6 and YbB_6 . The doublet spectra are understood by the two-dimensional charge distribution on B_6 without lattice distortion. In addition, the scattered intensities of the phonons change at around the ferromagnetic Curie temperature for YbB_6 and at $T \approx 600$ K for CaB_6 . These are the characteristic temperatures due to the change of the electronic system.

© 2003 Elsevier Inc. All rights reserved.

PACS: 78.30.-j; 75.50D; 71.20.Nr

Keywords: Raman scattering; Ferromagnetism; CaB_6 ; YbB_6 ; Anisotropic charge distribution of B_6

1. Introduction

Young et al. have reported ferromagnetism in a La doped Ca hexaboride with a small La concentration, which has high Curie temperature in spite of a small magnetic moment [1]. Ferromagnetism has been observed even in the host crystal of CaB_6 and in CaB_2C_2 [2]. However, recent experimental results claim that ferromagnetism of CaB_6 and CaB_2C_2 originated from the small amount of iron compounds at the surface and also the disappearance of ferromagnetism has been already reported for the surface-removed $\text{Ca}_{0.995}\text{La}_{0.005}\text{B}_6$ by Kunii [3]. However, the possibility of ferromagnetism is not completely excluded for CaB_6 , because the observation of ferromagnetic transition at 150 K has been reported for $\text{Yb}_{1-x}\text{La}_x\text{B}_6$ ($0 \leq x \leq 0.006$), where YbB_6 with a completely filled f^{14} shell is diamagnetic [4].

The appearing mechanism of ferromagnetism in these crystals is quite different from a conventional one, since the crystals do not contain transition elements. For the

theoretical approaches, two different models have been proposed: dilute electron gas model [5] and the exciton condensate model [6]. In the latter model, the band calculation concluded the existence of the overlap of the electron- and hole branches at X-point in Brillouin zone. This overlap suggests two-dimensional distortion of electronic system.

According to the report by Akimitsu [2], the similar properties between the CaB_2C_2 and CaB_6 suggest that the crystal structure of CaB_6 is slightly distorted from cubic structure to tetragonal one. Therefore, to check the distortion, the measurement of the symmetry-sensitive method is necessary. In this study, Raman scattering measurements have been employed to clarify whether CaB_6 is distorted or not.

2. Experimental

The samples of the present study were prepared by the following methods. Polycrystalline samples of CaB_6 were grown by a solid-state reaction of CaO and B powder. The powder mixtures were pressed into pellets and sintered at 1650°C for 2.5 h in the reduction

*Corresponding author. Fax: +81-824-24-0757.

E-mail address: nogita@hiroshima-u.ac.jp (N. Ogita).

atmosphere. The sample characterization was done by a powder X-ray diffraction, and the obtained patterns have confirmed the single phase of the cubic hexaboride structure. The Curie temperature of CaB_6 was 650 K, determined by the magnetic susceptibility measurements.

The single crystal YbB_6 was grown by a floating-zone method using an imagefurnace with four Xe lamps [7]. Other single crystals of RB_6 ($R = \text{Pr}, \text{Ce}$) were grown by a floating-zone method [8].

Raman scattering spectra were measured by the following multichannel detection systems. An Ar ion laser operated at 514.5 nm with an output power of 10 mW was used. We employed two different measurements: the so-called macro- and micro-Raman systems. The scattered light was analyzed by a triple monochromator, and the analyzed light was detected by a liquid N_2 cooled CCD detector. In order to avoid a local heating due to the incident beam, a He gas was employed for both measurements of high and low temperatures.

Three phonons are Raman-active for the hexaborides with the cubic symmetry: $A_{1g} + E_g + T_{2g}$. These vibrations are due to only B atoms (Fig. 2(c)), because Ca atom is located on an inversion center. The assignment of observed phonons is given by the following polarization dependence. A_{1g} appears in the (x, x) geometry, E_g in (x, x) and $(x + y, x - y)$, and T_{2g} in (x, y) , where x and y correspond to $[100]$ and $[010]$ axes, respectively. According to the theory [2,6], the most plausible symmetry is tetragonal. In this symmetry, the E_g mode in the cubic phase becomes $A_{1g} + B_{1g}$.

3. Results and discussion

Fig. 1 shows the Raman spectra of RB_6 ($R = \text{Ca}, \text{Yb}, \text{Ce}, \text{and Pr}$) measured at room temperature. The geometry of the presented spectra is $(x + y, x + y)$, where all Raman-active phonons in the cubic symmetry appear. The valence of cation R for the upper two spectra of CaB_6 and YbB_6 is divalent, and that for the lower two spectra of CeB_6 and PrB_6 is trivalent. The figure gives us the following remarkable difference between the divalent and trivalent cation crystals; the line shape of the E_g mode, the additional peak at about 1400 cm^{-1} marked by asterisks, crystal-electric-field (CEF) excitations (arrows), and anomalous low energy excitations (triangles). The E_g peak is doublet for only the divalent crystals, while that is a very broad single-peak for the trivalent ones. The other features of the peak at 1400 cm^{-1} , CEF and anomalous low energy excitations are observed for RB_6 with the trivalent crystals. In addition, the line shape of the T_{2g} peak is asymmetric for rare-earth hexaboride with the trivalent cation. For the CEF and anomalous excitations

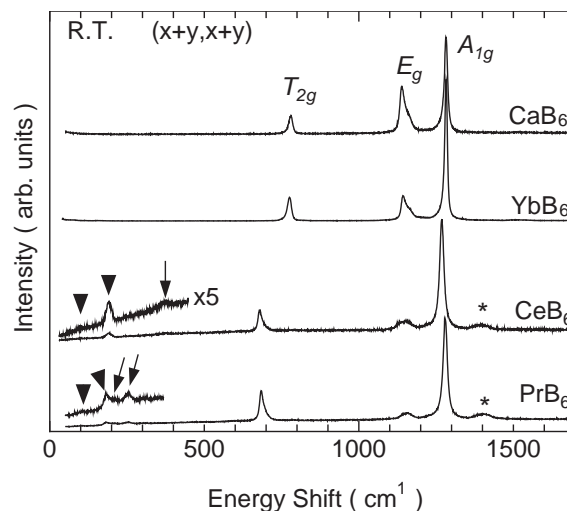


Fig. 1. Raman scattering spectra of RB_6 ($R = \text{Ca}, \text{Yb}, \text{Ce}, \text{and Pr}$) at room temperature in the $(x + y, x + y)$ geometry. The asterisks, arrows, and triangles are the additional peak, CEF excitations, and anomalous low energy excitations, respectively.

observed below 500 cm^{-1} , the detailed discussions will be reported elsewhere [9]. In this paper, we report about the high-energy excitations above 500 cm^{-1} .

It is well known that trivalent rare-earth hexaborides are monovalent metals. Actually, LaB_6 is one of the most typical monovalent metal [10]. SmB_6 is a semiconductor and special compound since the $4f^6$ and $4f^5$ configurations in the Sm ions ($4f^6 : 4f^5 \approx 3 : 7$) [11–13]. On the other hand, non-magnetic divalent rare-earth hexaborides such as YbB_6 are known as a typical narrow gap semiconductor [14]. These properties are in good agreement with the band calculation [15]. Therefore, the spectral difference between the divalent and trivalent-cation hexaborides is caused by the difference of electronic states.

Fig. 2 shows the polarization dependence of the Raman scattering spectra of CaB_6 and YbB_6 at room temperature. The spectra of CaB_6 were measured by the micro-Raman scattering from the rectangular-shaped micro-crystal, $20 \times 10 \mu\text{m}$. By this polarization dependence, three strong peaks are assigned as phonon and their corresponding irreducible representations are also depicted in the figures. As described above, if the doublet peak is due to tetragonal symmetry of CaB_6 , the E_g mode should change to the $A_{1g} + B_{1g}$ symmetry. However, the polarization dependence clearly shows that both doublet peaks at $\sim 1150 \text{ cm}^{-1}$ have the symmetry of E_g . Thus, the doublet peak of the divalent crystals is not caused by the change of the crystal symmetry.

An isotope effect of B^{10} and B^{11} is expected as one possible origin of the doublet structure. We have evaluated the possibility of the selective isotope ordering of B by the simple normal mode analysis, using the reported force constants by Takegahara and Kasuya

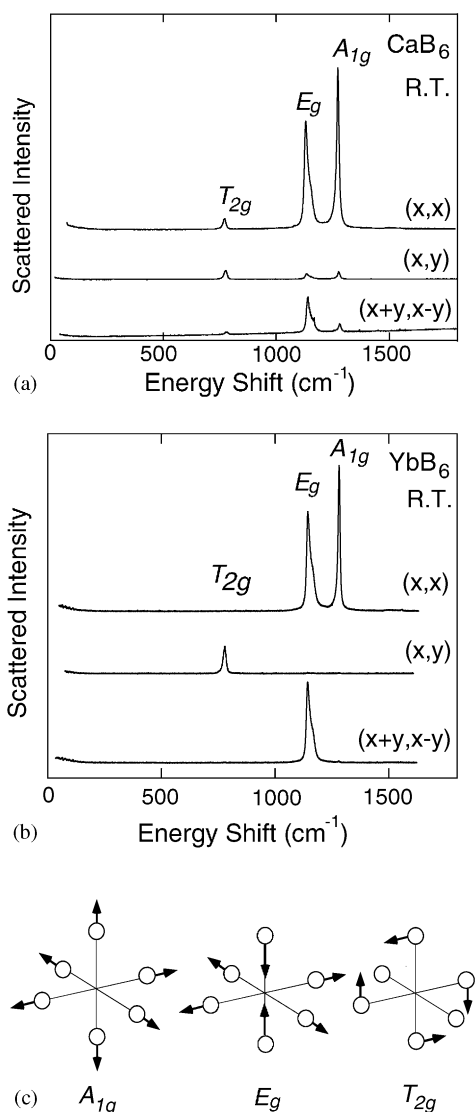


Fig. 2. Polarization dependence of Raman scattering spectra of (a) CaB_6 and (b) YbB_6 at room temperature. (c) Ionic displacement of three Raman-active phonons in the cubic symmetry.

[16]. We have obtained that such ordering increases the energy by $20\text{--}30\text{ cm}^{-1}$ for all phonon modes. Thus, the doublet of E_g is not caused by such isotope ordering.

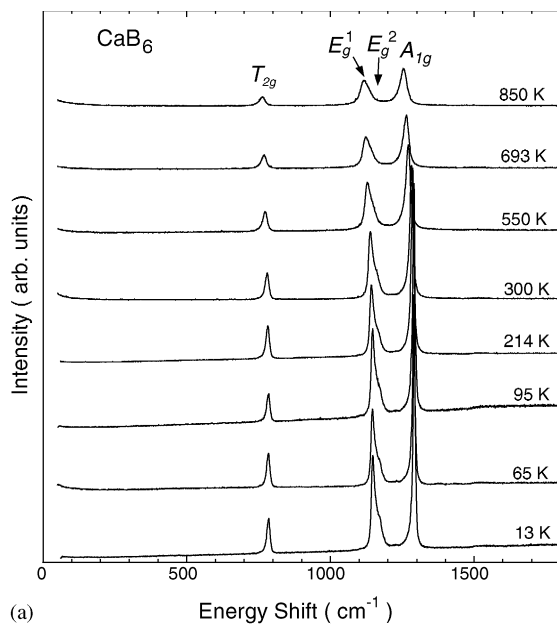
The atomic displacement of the Raman-active phonons in the cubic symmetry is shown in Fig. 2(c). The E_g mode is quite different from the other phonons, that is, the displacement of two apical-B atoms is twice of that of four planar-B atoms, while that is the same for A_{1g} and T_{2g} . Such displacement of E_g works as the anisotropic pressure for the B_6 octahedron. We label two E_g peaks by E_g^1 and E_g^2 for the lower- and higher-energy peaks, respectively. The experimental evidence of the doublet structure of the E_g peak confirms the existence of different force constants caused by the anisotropic charge distribution. If the charge distribution on B_6 is two-dimensional pancake, such charge

distribution will affect on E_g strongly and on T_{2g} slightly. In fact, the spectral shape of T_{2g} is slightly doublet at low temperature. Furthermore, the intensity ratio of E_g^1 to E_g^2 ($I(E_g^1)/I(E_g^2) \approx 2$) supports the two-dimensional charge distribution on B_6 . Thus, from the above discussions, the Raman scattering results of the divalent hexaborides CaB_6 and YbB_6 suggest that the electronic distribution of B_6 is the two-dimensional pancake type without lattice distortion.

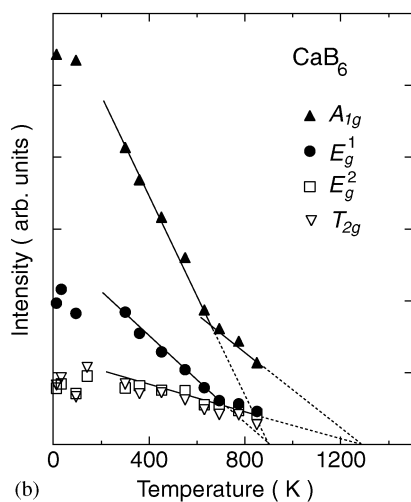
To check this possibility, the Rietveld analysis has been made for two models; isotropic charge distribution on B_6 molecule (cubic case) and anisotropic distribution with slightly two-dimensional distortion (tetragonal one). The obtained profile R -factor R_p was 6.43 and 6.35 for the cubic and the tetragonal case, respectively. However, among several R factors, we have found the better R factor for the cubic case than that for the tetragonal one. At this stage, it is hard to judge which model is appropriate by the Rietveld analysis. To determine the final charge distribution, precise measurement of X-ray analysis using single crystals is necessary.

Temperature dependence of Raman scattering spectra of CaB_6 is shown in Fig. 3(a) in the temperature region between 13 and 850 K. The presented spectra are regarded as the average spectra of many micro-crystals, since these spectra were measured by the macro-Raman system. To see the temperature dependence quantitatively, the symmetric lorentzian fitting has been made for E_g^1 , E_g^2 and A_{1g} . The energy and line width of the phonons gradually change. However, as shown in Fig. 3(b), the intensities of A_{1g} and E_{1g} show the slope-change around $T \approx 600$ K. We note here that the same results have been obtained for the other sample with a very small amount of ferromagnetism (0.033 emu/mol at 5 K). Thus, the obtained phenomena are regarded as the intrinsic property of CaB_6 . The results for YbB_6 are shown in Fig. 4. The energy and line width also gradually change like CaB_6 . As shown in Fig. 4(b), the peak intensity changes around 150 K for YbB_6 , not at 600 K. The temperature of 150 K coincides with the ferromagnetic transition temperature of YbB_6 reported by Iga et al. [4]. The intensity change gives us the following knowledge. The change of the intensities suggests the change of the electronic polarizability or electronic state, because the Raman intensity is proportional to the square of the electronic polarization induced by the incident laser.

In the trivalent crystals, the above intensity change has not been found and the broad single peak of E_g suggests that the charge distribution is isotropic. Thus, for the present phenomena for divalent hexaborides, the two-dimensional charge distribution is important. As the related experimental evidence of the characteristic electronic distribution, we can point out the recent results of the photoemission experiment. Tohoku group and the Allen group observed the electron pocket at



(a)



(b)

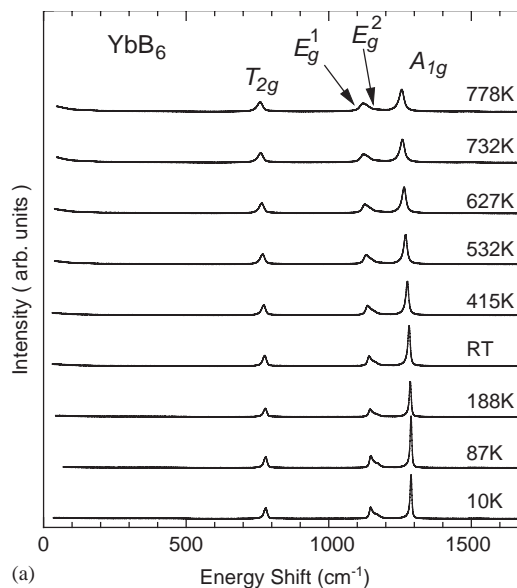
Fig. 3. Temperature dependence of (a) the phonon spectra, and (b) the peak intensities of CaB_6 .

X-point, instead of the overlap of electron and hole branches [17,18].

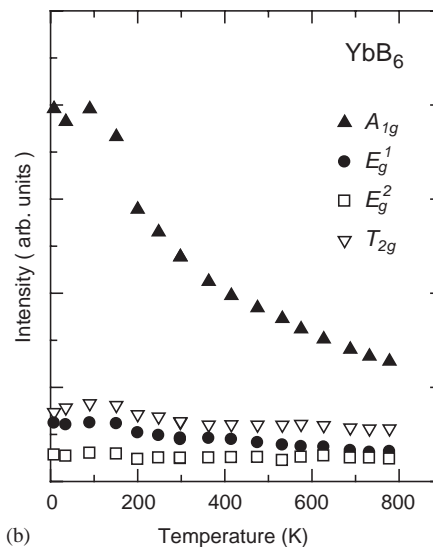
In the relationship with ferromagnetism, we have found the good correlation for YbB_6 , as described above. For CaB_6 , the recent experimental research is suspicious for the high Curie temperature. It is not easy to conclude the correlation for CaB_6 , however, the change of electronic state occurs at around 600 K even for the samples with very small ferromagnetism. The microscopic origin of the change of electronic state is the remaining problem.

4. Conclusion

Temperature and polarization dependence of Raman scattering spectra of CaB_6 , YbB_6 , and trivalent hex-



(a)



(b)

Fig. 4. Temperature dependence of (a) the phonon spectra, and (b) the peak intensities of YbB_6 .

aborides have been measured. From the observation of the doublet E_g peak and the change of peak intensity in the divalent hexaborides of CaB_6 and YbB_6 , it has been concluded about the existence of the anisotropic charge distribution without lattice distortion and the change of charge distribution on B_6 . The appearance of ferromagnetism may be correlated to this charge distribution of B_6 .

Acknowledgments

This work is supported in part by a Grant-in-Aid for COE Research (No. 13CE2002) of the Ministry of Education, Culture, Sports, Science and Technology of

Japan. The low temperature experiments is supported by the cryogenic center of Hiroshima University.

References

- [1] D.P. Young, D. Hall, M.E. Torelli, Z. Fisk, J.L. Sarrao, J.D. Thompson, H.-R. Ott, S.B. Oseroff, R.G. Goodrich, R. Zysler, *Nature* 397 (1999) 412–414.
- [2] J. Akimitsu, K. Takenawa, K. Suzuki, H. Harima, Y. Kuramoto, *Science* 293 (2001) 1125–1127.
- [3] S. Kunii, *J. Phys. Soc. Jpn.* 68 (1999) 3189–3190.
- [4] F. Iga, Y. Ueda, T. Takabatake, T. Suzuki, W. Higemoto, K. Nishiyama, H. Kawanaka, *Phys. Rev. B* 65 (2002) 220408(R) 1–4.
- [5] D. Ceperley, *Nature* 397 (1999) 386–387.
- [6] M.E. Zhitomirsky, T.M. Rice, V.I. Anisimov, *Nature* 402 (1999) 251–253.
- [7] F. Iga, N. Shimizu, T. Takabatake, *J. Magn. Magn. Mater.* 177–181 (1998) 337–338.
- [8] S. Kunii, *J. Phys. Soc. Jpn.* 57 (1988) 361–366.
- [9] N. Ogita, S. Nagai, N. Okamoto, M. Udagawa, F. Iga, M. Sera, J. Akimitsu, S. Kunii, *Physica B*, to be published.
- [10] Y. Ishizawa, T. Tanaka, E. Bannai, S. Kawai, *J. Phys. Soc. Jpn.* 42 (1977) 112–118.
- [11] E.E. Vainshtein, S.M. Blokhin, Yu.B. Paderno, *Sov. Phys. Solid State* 6 (1965) 2318–2320.
- [12] A. Menth, E. Buehler, T.H. Geballe, *Phys. Rev. Lett.* 22 (1969) 295–297.
- [13] R.L. Cohen, M. Eibschütz, K.W. West, *Phys. Rev. Lett.* 24 (1970) 383–386.
- [14] J.M. Tarascon, J. Etourneau, P. Dordor, P. Hagenmuller, M. Kasaya, J.M.D. Coey, *J. Appl. Phys.* 51 (1980) 574–577.
- [15] A. Hasegawa, A. Yanase, *J. Phys. F* 7 (1977) 1245–1260.
- [16] K. Takegahara, T. Kasuya, *Solid State Commun.* 53 (1985) 21–25.
- [17] S. Souma, T. Takahashi, Y. Umeda, N. Kimura, S. Kunii, H. Aoki, *J. Phys. Soc. Jpn.* 71 (Suppl.) (2002) 317–319.
- [18] J.D. Denlinger, J.A. Clack, J.W. Allen, G.-H. Gweon, D.M. Poirier, C.G. Olson, J.L. Sarrao, Z. Fisk, *cond-mat/0009022*.